



# Decomposition of oil cleaning agents from nuclear power plants by supercritical water oxidation

Shi-Bin Li<sup>1,2</sup> · Xiao-Bin Xia<sup>1</sup> · Qiang Qin<sup>1,2</sup> · Shuai Wang<sup>1</sup> · Hong-Jun Ma<sup>1</sup>

Received: 5 November 2021 / Revised: 19 January 2022 / Accepted: 3 March 2022 / Published online: 20 April 2022

© The Author(s), under exclusive licence to China Science Publishing & Media Ltd. (Science Press), Shanghai Institute of Applied Physics, the Chinese Academy of Sciences, Chinese Nuclear Society 2022

**Abstract** Oil cleaning agents generated from nuclear power plants (NPPs) are radioactive organic liquid wastes. To date, because there are no satisfactory industrial treatment measures, these wastes can only be stored for a long time. In this work, the optimization for the supercritical water oxidation (SCWO) of the spent organic solvent was investigated. The main process parameters of DURSET (oil cleaning agent) SCWO, such as temperature, reaction time, and excess oxygen coefficient, were optimized using response surface methodology, and a quadratic polynomial model was obtained. The determination coefficient ( $R^2$ ) of the model is 0.9812, indicating that the model is reliable. The optimized process conditions were at 515 °C, 66 s, and an excess oxygen coefficient of 211%. Under these conditions, the chemical oxygen demand removal of organic matter could reach 99.5%. The temperature was found to be the main factor affecting the SCWO process. Ketones and benzene-based compounds may be the main intermediates in DURSET SCWO. This work provides basic data for the industrialization of the degradation of spent organic solvents from NPP using SCWO technology.

**Keywords** Supercritical water oxidation · Oil cleaning agent · Nuclear power plants · Response surface methodology

## 1 Introduction

By the end of August 2021, 51 nuclear power units were in operation in mainland China. Each nuclear power unit produces approximately 1 m<sup>3</sup> of radioactive organic liquid waste annually, including radioactive oil waste and spent organic solvents. Radioactive oil waste primarily originates from the lubricating oil of the main circuit heat transfer pump, turbine oil, and hydraulic oil of the fuel loader. Spent radioactive organic solvents mainly come from the oil cleaning agents of equipment and metal parts and a small amount of liquid scintillation waste produced by laboratory analysis. Oil waste mainly consists of long-chain alkanes (mostly more than 20 carbon chains), and its activity is approximately 100–150 Bq m<sup>-3</sup>; spent organic solvents are mainly short-chain alkanes (9–12 carbon chains), and their activity is approximately 150 MBq m<sup>-3</sup> [1]. The major radionuclides are Co<sup>58</sup>, Co<sup>60</sup>, Cs<sup>134</sup>, Cs<sup>137</sup>, etc.

Different technologies have been used to dispose of radioactive organic solvents, including incineration [2, 3], adsorption–solidification [4, 5], wet oxidation [6], steam reforming [7], electrochemical oxidation [8], etc. Among these methods, the incineration method can effectively reduce the volume of the treatment effect, but the incineration process produces secondary pollution (such as NO<sub>x</sub>, SO<sub>x</sub>, and dioxins), which can easily cause equipment corrosion and low public acceptance. The wet oxidation method has a lower operating temperature and pressure, but

This work was supported by Shanghai Sail Program (No. 19YF1458000).

✉ Xiao-Bin Xia  
xi Xiaobin@sinap.ac.cn

<sup>1</sup> Shanghai Institute of Applied Physics, Chinese Academy of Sciences, Shanghai 201800, China

<sup>2</sup> University of Chinese Academy of Sciences, Beijing 100049, China

the reaction time is generally long, and some corrosion may be caused by the introduction of oxidants ( $\text{NO}_3^-$ ) [9] or heteroatoms (S and Cl). The adsorption–solidification method has advantages of a simple process and low cost, while the organic adsorption capacity and containment rate are low, and the nuclide is easily leached. Steam reforming technology has problems with equipment corrosion and high energy consumption. Owing to the lack of mature and safe treatment technology, radioactive organic waste liquid can only be temporarily stored, and long-term storage has the potential safety hazards of leakage and ignition. Consequently, new technologies must be developed to efficiently and safely treat waste.

Supercritical water oxidation (SCWO) is a promising green method for degrading organic structures in most organic wastes. At conditions exceeding its critical point ( $T > 374\text{ }^\circ\text{C}$ ,  $P > 22.1\text{ MPa}$ ), there are quite a few advantages in supercritical water (SCW), such as low viscosity, low dielectric constant, high diffusion coefficient, and low ionization constant [10, 11]. SCW is miscible with most organics and non-polar inorganic molecules, such as oxygen and carbon dioxide, to form a homogeneous reaction environment, thereby reducing the mass transfer resistance and improving the reaction rate [12]. Because refractory organics can be quickly and completely degraded by SCWO, the process does not produce hazardous emissions, such as  $\text{NO}_x$ ,  $\text{SO}_x$ , and dioxins. In addition, there is almost no volatilization of radioactive metal nuclides [13].

Considering these advantages, SCWO has been widely applied to treat various refractory organic wastewaters, such as pharmaceutical wastewater [14, 15], semi-coke wastewater [16], explosive wastewater [17], landfill leachate [18], and pesticide wastewater [19]. Moreover, a corresponding industrial wastewater treatment device has been built and operated [20]. Research on the SCWO treatment of radioactive organic waste has mainly focused on tributyl phosphate (TBP) [21] and ion exchange resin [22]. Golmohammadi et al. [23] investigated the oxidation reaction kinetics of TBP in SCW with different temperatures ranging from 370 to 480  $^\circ\text{C}$ . The use of  $\text{Fe}_2\text{O}_3$  catalyst in the experiment greatly improved total organic carbon (TOC) removal by 20%. Furthermore, according to the experimental results, the in-depth mechanism of supercritical water catalytic oxidation of TBP was summarized and analyzed, and the main intermediate products were dibutyl phosphate, monobutyl phosphate, and butyric acid [24]. Leybros et al. [25] studied the degradation mechanism of SCWO treatment of radioactive waste ion resin.  $\text{HOO}$  radicals participate in the process of polymer decomposition to generate aromatic acids and alcohols. The main intermediate compounds are benzoic acid, phenol, and acetic acid. Wang et al. [26] performed

gasification of cationic ion exchange resin in SCW using a batch reactor. The carbon gasification efficiency was up to 97.98% with  $\text{K}_2\text{CO}_3$  added and 30 min at 750  $^\circ\text{C}$ , and liquid products were mainly composed of benzene, monocycle arenes, phenol groups, and polycyclic aromatic hydrocarbons. In previous research, we studied the oxidative degradation of a radioactive spent extraction solvent in SCW [13, 27]. Results showed that the TOC removal rate of organic matter can reach 99.5%. In addition, it has been revealed that the solubility of radioactive inorganic salts in SCW is helpful in understanding the deposition characteristics of the reaction [28]. Additionally, SCWO treatment of lubricating oil in nuclear power plants has also been studied [29]. The results showed that the optimal reaction conditions were temperature of 550  $^\circ\text{C}$ , a reaction time of 80 s, an excess oxygen coefficient of 250%, and a removal rate of organic matter of up to 96%. According to the previous literature, it is worth emphasizing that supercritical water oxidation has unique advantages in the treatment of radioactive organic waste. However, no basic research on the treatment of spent radioactive organic solvents from nuclear power plants using SCWO technology has been conducted. The spent radioactive organic solvent is oxidized by supercritical water, converted into radioactive wastewater, and then treated with mature technologies such as evaporation, precipitation, or ion exchange to meet the emission standards [1].

In this study, SCWO technology was used to optimize the reaction conditions of oil cleaning agent simulants, improve the efficiency of organic removal, and realize harmless treatment of radioactivity. The DURSET was selected as the test object for SCWO. First, through single-factor experiments, the main influencing factors and value ranges were determined for SCWO. The effects of different factors and interactions on the chemical oxygen demand (COD) removal of organic matter in SCW were investigated using response surface methodology (RSM). Subsequently, a quadratic polynomial model was established between independent factors and responses. The best operating parameters were then obtained through an optimization analysis. Finally, verification experiments were conducted to confirm the reliability of the model. In addition, the main components of the reaction products in the SCW were analyzed.

## 2 Materials and methods

### 2.1 Materials

Hydrogen peroxide ( $\text{H}_2\text{O}_2$ , 30%, w/w) was purchased from Sinopharm Chemical Reagent Co. (China). The DURSET cleaning agent (PSC-002) was purchased from

the NCH HUYANG Co. (Dalian, China). The physicochemical properties of the DURSET are listed in Table 1. The measured value of COD was  $6.20 \times 10^5 \pm 3.7\%$  mg·L<sup>-1</sup>, which was used to calculate the required amount of hydrogen peroxide oxidizer for fully oxidizing DURSET using stoichiometric method. The density, pH, flash point, and saturated aliphatic hydrocarbons were obtained from the product details. The GC–MS chromatogram and main components of DURSET are shown in Fig. 1 and Table 2, respectively. It can be seen that the main components of the stock solution are monocyclic alkanes (1,2,4-trimethylcyclohexane, 1,2,3-trimethylcyclohexane, 2-cyclohexylbutane, etc.) and bicyclic alkanes (decalin, 2-methyldecalin, etc.). In addition, it contains a small number of refractory monocyclic aromatic hydrocarbons.

## 2.2 Apparatus and procedure

The SCWO-1000 system was constructed based on the SCWO-250 system used in the previous studies [13, 27], as shown in Fig. 2. The reaction system mainly included one tank reactor (1000 mL, Inconel 625) and two preheaters (200 mL and 250 mL, Inconel 625). The maximum operating temperature and pressure of the equipment were 600 °C and 28.4 MPa, respectively. Considering that pressure had no significant effect on organic matter removal, all experiments were performed at 24 MPa. Before the start of each SCWO experiment, deionized water was pumped into two preheaters and one tank reactor, and the temperature was gradually increased using the PID meter (proportional integral derivative). When the internal temperature exceeded 100 °C, the pressure should be slowly increased to the expected value. Deionized water and a hydrogen peroxide solution were jointly pumped into the preheaters via a pressure metering pump (pump 1). Then, the feedstock solution (DURSET) was pumped directly into the tank reactor with the assistance of another pressure metering pump (pump 2). After the exothermic SCWO reaction, the outflowing reaction mixture was cooled to room temperature using a tubular cooling device. The condensed reaction mixture was adjusted to atmospheric pressure using a backpressure regulator (BPR). The mixture was sent to a gas–liquid separator, and the required liquid product sample was obtained after separation of the gas and liquid. The organic matter content in the liquid effluents was measured and evaluated using a HACH

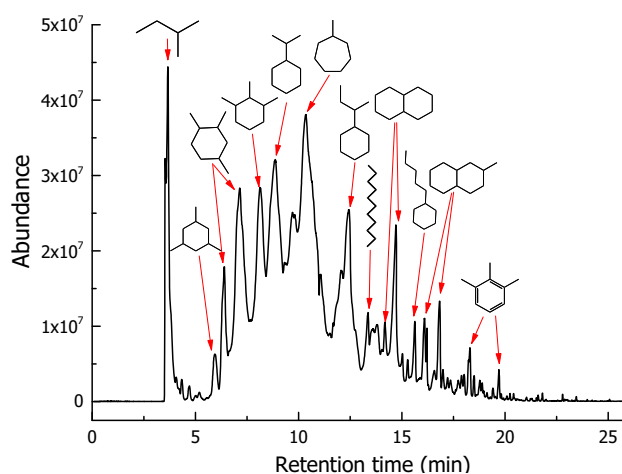


**Fig. 1** GC–MS chromatogram of DURSET

chemical oxygen demand digestion reactor and colorimeter.

## 2.3 Analysis methods

The main ingredients of DURSET and liquid effluent were analyzed by gas chromatography/mass spectrometry (GC7890A/MS5975C, Agilent, USA) with a HP-INNO-WAX capillary column (60 m × 0.25 mm I.D., 0.25 μm film thickness). Helium (1 mL/min) was used as carrier gas. The temperature program of the oven was as follows: isothermal at 40 °C for 5 min, ramped up to 100 °C at 5 °C/min, and ramped up to 230 °C at 10 °C/min, and held for 15 min. The working voltage of the MS ion source (EI) was 70 eV, and its working temperature was 230 °C. 150 °C was used as the operating temperature of the MS quadrupole.

The COD values of DURSET and the liquid products were determined by rapid digestion spectrophotometry (HJ/T399–2007). The measuring equipment used was the digestion device (DRB 200, HACH, USA) and portable spectrophotometer (HACH, DR 890, USA). First, 2 mL of the liquid product sample was injected into a digestion tube (in the range of 0–1500 mg·L<sup>-1</sup>). Then, the digestion tubes were placed into the digestion reactor for the digestion reaction for two hours at 150 °C. Finally, the COD values were measured using a portable spectrophotometer. To ensure the credibility and accuracy of the COD measured by DURSET, a dilution measurement method was adopted to conduct six parallel experiments.

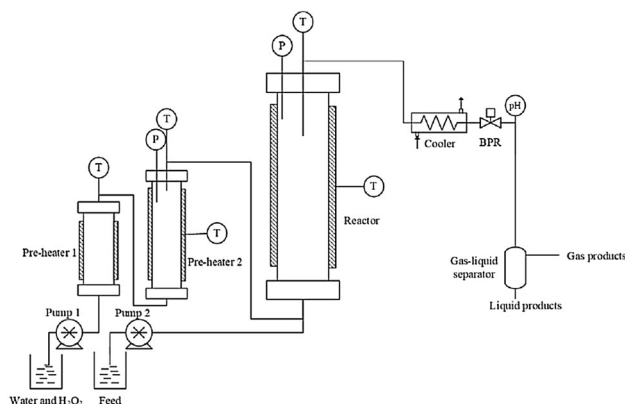
**Table 1** Physicochemical properties of DURSET

COD (mg·L <sup>-1</sup> )*	Density (kg·L <sup>-1</sup> )	pH	Flash point (°C)	Saturated aliphatic hydrocarbon (wt%)
$6.20 \times 10^5 \pm 3.7\%$	0.75	7	48	80–90

\*COD value was determined by rapid digestion spectrophotometry

**Table 2** Main components of DURSET

Composition	Monocyclic alkanes	Bicyclic alkanes	Linear alkanes	Monocyclic aromatics	Other substances
Percentage (wt%)	69.41	14.21	4.96	2.08	9.34

**Fig. 2** Schematic diagram of SCWO system (T: Temperature meter, P: Pressure gage)

The COD removal efficiency (CRE, %) of the liquid effluent was calculated using the following formula:

$$\text{CRE} = \frac{[\text{COD}]_0 - [\text{COD}]_L}{[\text{COD}]_0} \times 100\%, \quad (1)$$

where  $[\text{COD}]_0$  represents the concentration of chemical oxygen demand in the feedstock after considering the dilution influence of deionized water and hydrogen peroxide solution and  $[\text{COD}]_L$  represents the concentration of chemical oxygen demand in the liquid effluent.

The excess oxygen coefficient ( $\alpha$ , %) is calculated using the following equation:

$$\alpha = \frac{[\text{O}_2]_r - [\text{O}_2]_0}{[\text{O}_2]_0} \times 100\%, \quad (2)$$

where  $[\text{O}_2]_0$  is the concentration of oxidant needed to completely oxidize the organic substances calculated in accordance with the theoretical stoichiometric ratio,  $[\text{O}_2]_r$  is the actual concentration of oxidant during each reaction test.

The reaction time ( $t$ , s) refers to the residence time in the reactor, and is defined as follows:

$$t = 60 \times \frac{V_0}{Q} \times \frac{V}{V_r}, \quad (3)$$

where  $V_0 = 1000$  mL is the volume of the tank reactor,  $V$  and  $Q$  imply the specific volume and rate of volumetric flow from the liquid product at room temperature and atmospheric pressure, respectively, and  $V_r$  implies the

specific volume of feedstock under the conditions of the oxidation reaction.

## 2.4 Experimental model design

Response surface methodology (RSM) was used to design the experimental scheme for SCWO of DURSET, which was based on the CCD principle (central composite design). Design Expert software version 8.0.6 (Stat-Ease, Inc., Minneapolis, MN, USA) was used for the design. The application of statistical auxiliary tools can reduce material consumption and expenses. This is mainly due to the reduction in working hours and number of experiments. In addition, the scheme design can establish a multiple equation model between each independent factor and the response value. It can also optimize the model to reveal the multiple, interactive, and linear influences between the independent factors and response values.

Before designing the response surface scheme, it was necessary to determine the main influencing factors and range through single-factor experiments. In this study, the feed concentration ( $C$ , 1.5–3.0 wt.%), temperature ( $T$ , 440–580 °C), reaction time ( $t$ , 30–105 s) and excess oxygen coefficient ( $\alpha$ , 50–300%) were selected as influencing factors, which affected COD removal of DURSET via SCWO. Next, the influence of reaction parameters was analyzed through single-factor experiments. Finally, the central selection points of the main influencing factors, such as the temperature, reaction time, and excess oxygen coefficient, were determined (see Sect. 3.1).

Subsequently, the set pressure and feed concentration were set to 24 MPa and 2 wt%, respectively. The influences of temperature, reaction time, and excess oxygen coefficient were studied using the experimental method of central composite design (CCD) of three factors and five levels. The levels and ranges of the independent factors are tabulated in Table 3. The CCD is mainly suitable for multi-factor and multi-level experiments, usually with five levels for each factor. The interaction between these significant factors can be intuitively determined, and the optimal reaction conditions can be obtained using a high-precision quadratic regression equation. The total number of experimental tests is expressed by the formula [30]:

**Table 3** Range and levels of independent factors

Factors	Symbol	Range and levels of independent factors				
		-2	-1	0	1	2
Temperature (°C)	$T$	430	460	490	520	550
Reaction time (s)	$t$	25	40	55	70	85
Excess oxygen coefficient (%)	$\alpha$	50	100	150	200	250

$$N_T = 2^k + 2k + c, \quad (4)$$

where  $k$  is the number of influencing factors and  $c$  is the number of center points. A total of 20 tests were applied to this RSM design, of which there were six axial points, eight factorial points, and six repeated experiments at the center point. The relationship between the independent variable and the response value was regressed using a multiple model equation [31]. This is expressed by the following equation:

$$Y = \beta_0 + \sum \beta_i X_i + \sum \beta_{ii} X_i^2 + \sum \beta_{ij} X_i X_j + \varepsilon, \quad (5)$$

where  $Y$  is the expected response value,  $X_i$  is the independent variable,  $\beta_0$  is a constant value of the model,  $\beta_i$  is the coefficient of linear variables,  $\beta_{ii}$  is the coefficient of quadratic variables,  $\beta_{ij}$  is the coefficient of interactive variables, and  $\varepsilon$  is the residual random error in the test.

Finally, the reliability of the response surface model was assessed by analyzing  $R^2$  (coefficient of determination) and  $R^2_{\text{adj}}$  (adjusted value). Subsequently, the significance of the quadratic model equation was verified by analysis of variance (including the  $P$ -value,  $F$ -value, and coefficient of variation).

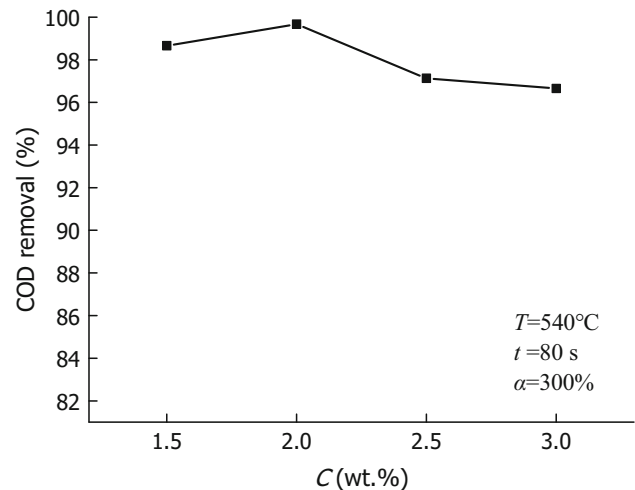
### 3 Results and discussion

#### 3.1 Single-factor experiment on COD removal efficiency

All the experiments were performed at approximately 24 MPa. In this section, the effects of feed concentration, temperature, reaction time, and excess oxygen coefficient on the CRE were studied. The optimal range of the main factors in the response surface experiments was selected through single-factor experiments.

##### 3.1.1 Effect of feed concentration on CRE

Figure 3 presents the influence of feed concentration of DURSET on COD removal in SCWO at 540 °C, a reaction time of 80 s, and excess oxygen coefficient 300%. As shown in Fig. 3, when the feed concentration increased from 1.5 to 2.0 wt%, the CRE increased from 98.66 to

**Fig. 3** Effect of feed concentration on COD removal efficiency

99.67%. However, when the content exceeded 2 wt%, there was a relative downward trend. When the feed concentration increased and the organic removal rate decreased, the COD of the liquid effluent tended to increase. Moreover, a high feed concentration may lead to an increase in second-order polymerization reactions, resulting in char and tar byproducts [32]. In general, the feed concentration of the reactants had no significant effect on the COD removal. Consequently, the effect of feed concentration was not considered in subsequent response surface experiments.

##### 3.1.2 Effect of temperature on CRE

The CRE of DURSET was significantly affected by the temperature, as shown in Fig. 4. The CRE gradually increased with increasing temperature at a feed concentration of 2 wt%, reaction time of 55 s and excess oxygen coefficient of 300%. When the temperature increased from 440 to 540 °C, the CRE clearly increased from 88.75 to 99.41%. However, the CRE only increased by approximately 0.40% when the temperature increased from 540 to 580 °C. Accordingly, when the temperature was relatively low, an increase in temperature was an effective measure to quickly increase the COD removal of organic matter. This may be due to the increase in temperature, which helped trigger molecular activity in the supercritical water reaction



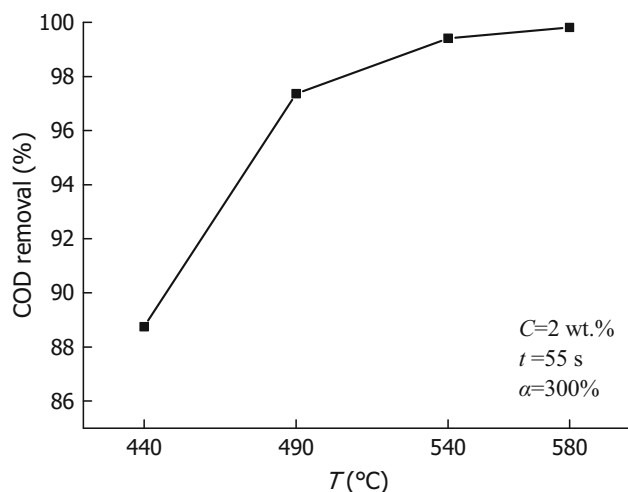


**Fig. 4** Effect of temperature on COD removal efficiency

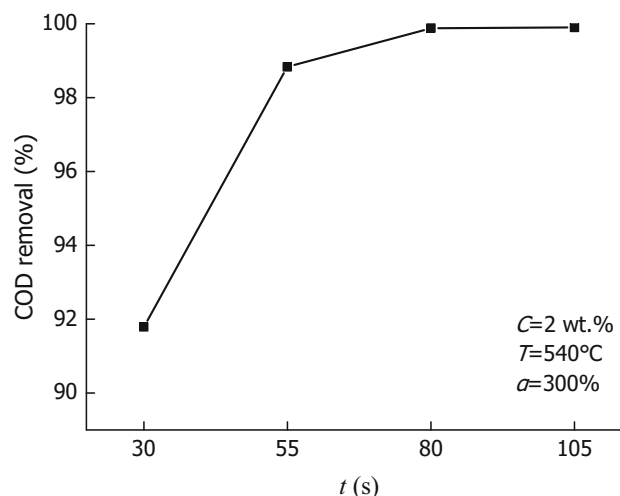


**Fig. 5** Effect of reaction time on COD removal efficiency

system. Yang et al. [33] studied the decomposition of 15 aromatic compounds in supercritical water oxidation at 350–550 °C. The results indicate that temperature played an important role in the removal of various organic matter in the SCWO. Al-Duri et al. [34] conducted an experimental study on the SCWO degradation of nitrogenous hydrocarbons 1,8-diazobicyclo [5.4.0] undec-7-ene (DBU). It was found that at the conditions of oxidant stoichiometric ratio of 200%, pressure of 25 MPa, and residence time of 7 s, the TOC removal rate increased from about 17 to 98% when the temperature increased from 400 to 525 °C, which showed that the effect of temperature was very significant. In this work, to obtain a fitted quadratic model with a wide temperature range, a temperature range of 430–550 °C was used of the response surface experiment, and a temperature of 490 °C was selected as the center point.

### 3.1.3 Effect of reaction time on CRE

The effect of reaction time from 30 to 105 s on the COD removal of the SCWO process at a feed concentration of 2 wt%, temperature of 540 °C, and excess oxygen coefficient of 300% is shown in Fig. 5. Figure 5 shows that under the given conditions, the CRE obviously grew from 91.79 to 99.90%. The CRE increased rapidly with increasing reaction time in the range of 30–55 s, after which the increasing trend slowed with depleted reactants. This result may be explained by the free-radical reaction mechanism in a supercritical water environment [35]. Bühler et al. [36] reported that OH·- and H·-free radicals play a key role in the degradation of organic molecules in SCW. Yu et al. [37] studied the treatment of oily wastewater using SCWO and concluded that when the

reaction time increased from 1 to 9 min, the COD removal rate approximately increased from 69 to 78%. At the same time, with the use of  $\text{Cu}^{2+}$  catalyst, the COD removal rate increased from 83 to 93%. Chen et al. [38] investigated the effect of the reaction time on SCWO degradation in oil-based drilling cuttings. At the condition of the reaction temperature 500 °C and oxidation coefficient 250%, the TOC removal rate increased by 25% when the reaction time increased from 30 to 120 s. These results show that the effect of reaction time plays a significant role in SCWO. Hence, a reaction time of 55 s was selected as the response surface center design point, while the reaction time ranged from 25 to 85 s.

### 3.1.4 Effect of excess oxygen coefficient on CRE

The influence of excess oxygen coefficient in the range of 50–300% and at the conditions of a feed concentration of 2 wt%, 540 °C, and 80 s is given in Fig. 6. When the excess oxygen coefficient increased from 50 to 200%, the CRE clearly grew from 92.01 to 99.43%. When the excess oxygen coefficient exceeded 200%, the amount of oxidant had little effect on the CRE. This may be due to an excess of oxidant. Gong et al. [39] found that the TOC removal rate increased rapidly when the oxidation coefficient increased from 0 to 200% during SCWO degradation of quinazoline. When it exceeded 200%, the TOC removal rate plateaued to a constant value, which also confirmed our results to some extent. In addition, we found that if the excess oxygen coefficient was lower than 50%, a lot of insoluble black tar appeared in the liquid effluent, which could easily cause the reactor pipe to block. Related studies [32, 40] have pointed out that the precursor molecules of tars are polycyclic compounds, including naphthalene and

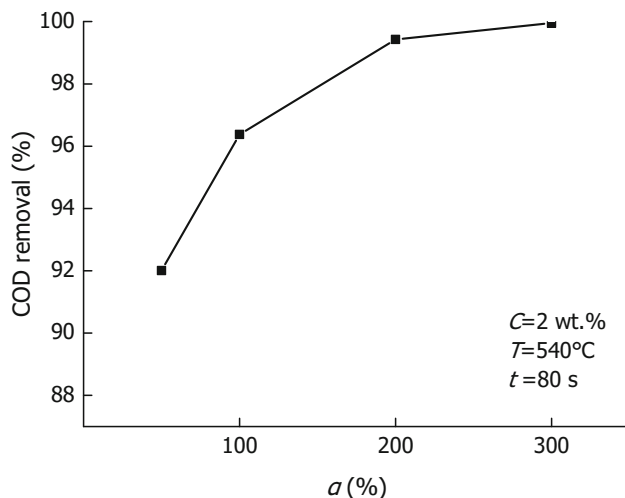


**Fig. 6** Effect of excess oxygen coefficient on COD removal efficiency

phenanthrene. Besides, Wahyudiono et al. [41] studied the liquefaction of tar in sub- and supercritical water and found that the main products from the liquefaction of tar were phenol, biphenyl, diphenyl ether, and diphenylmethane, respectively. This phenomenon may be due to the formation of intermediate compounds and their polymerization processes, which resulted in the production of tar and char [42]. Therefore, to reduce the production of tar, the range of excess oxygen coefficient was selected to be 50–250% in the response surface experiment.

### 3.2 Model fitting and ANOVA

The response surface method based on CCD was used to probe the effect of the process parameters on the SCWO of the oil cleaning agent. Table 4 shows the experimental results of the CCD assays for SCWO of DURSET. The results showed that there were significant differences in the CRE of the SCWO systems under different reaction conditions. Figure 7a shows a favorable linear correlation between the experimental and predicted values. Figure 7b presents the normal plot of residuals that shows that the points follow a linear regularity, which means that the error terms are normally distributed [43]. Therefore, the proposed model is credible.

Combined with the results in Table 4, which shows the experimental and predicted values of the three responses, an empirical relationship between the experimental variables and response is obtained using Eq. (6). In Eq. (6), the CRE was used as the response value, which was associated with the coded independent variables, including temperature, reaction time, and excess oxygen coefficient.

**Table 4** Design approach and experimental results of response surface methodology

Run	Variables			Responses	
	<i>T</i> (°C)	<i>t</i> (s)	<i>α</i> (%)	CRE (%)	
				Experimental	Predicted
1	490	55	150	95.01	95.61
2	490	55	50	90.05	90.42
3	490	55	150	95.74	95.61
4	490	55	150	96.18	95.61
5	430	55	150	84.01	83.70
6	490	55	250	96.86	96.26
7	490	55	150	96.36	95.61
8	460	40	200	89.32	89.23
9	460	40	100	87.53	87.09
10	520	40	200	95.34	95.19
11	460	70	100	88.89	89.28
12	460	70	200	90.53	91.52
13	490	85	150	95.88	94.81
14	550	55	150	96.96	97.04
15	490	55	150	95.31	95.61
16	520	40	100	92.35	91.59
17	520	70	100	96.33	96.65
18	520	70	200	99.68	99.99
19	490	25	150	86.61	87.45
20	490	55	150	95.29	95.61

$$\begin{aligned} \text{CRE}(\%) = & 95.56 + 3.33T + 1.84t + 1.46\alpha + 0.72Tt + 0.36T\alpha \\ & + 0.026t\alpha - 1.31T^2 - 1.12t^2 - 0.57\alpha^2 \end{aligned} \quad (6)$$

Analysis of variance (ANOVA) was used to verify the reliability of the model. The ANOVA of the fitted quadratic model for the SCWO process of DURSET is shown in Table 5. As shown in Table 5, a model *P*-value of less than 0.0001 indicated that the model was statistically significant. *P*-values less than 0.05 implied that the model terms were stable and significant [44]. In this case, the significant model terms were *T*, *t*, *α*, *Tt*, *T*<sup>2</sup>, *t*<sup>2</sup>, and *α*<sup>2</sup>, with corresponding *P*-values of < 0.0001, < 0.0001, < 0.0001, 0.0294, < 0.0001, < 0.0001, and 0.0052, respectively. In other words, temperature, reaction time, and excess oxygen coefficient, as well as the interaction between temperature and reaction time, significantly affected the CRE response. The model *F*-value of 57.84 meant the model was significant. It can be observed that the temperature with an *F*-value of 277.44 was a determinant of the reaction time and excess oxygen coefficient, with *F*-values of 84.49 and 53.37, respectively. Therefore, the order of factors

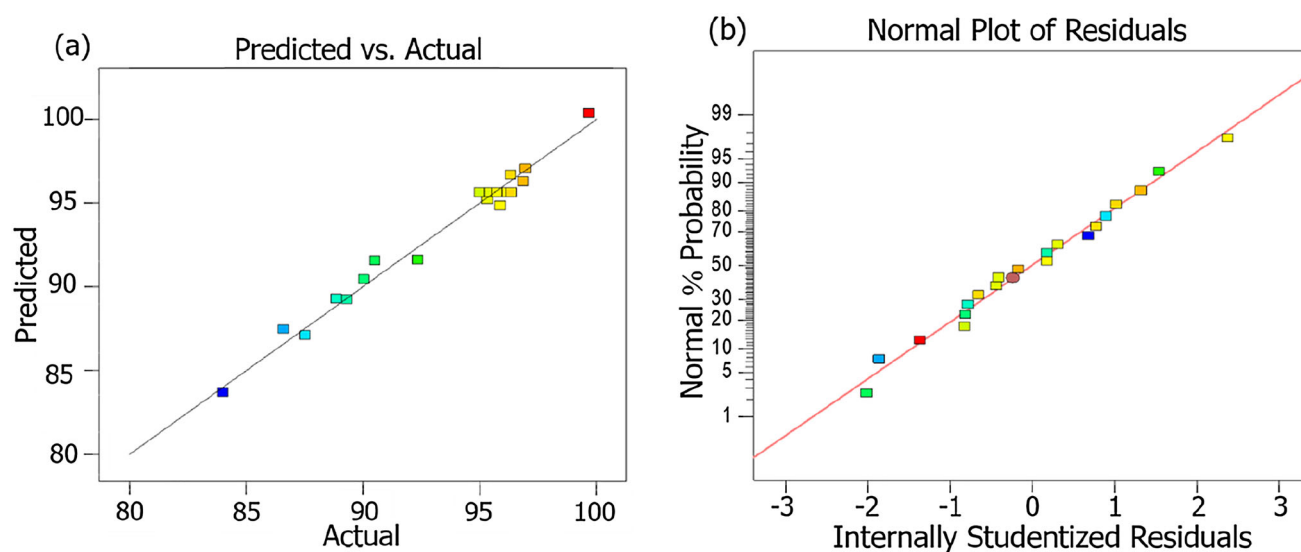


**Fig. 7** Comparison of **a** CRE obtained by the experiment values and model predicted. **b** Normal probability of internally studentized residuals for CRE

**Table 5** ANOVA results of the quadratic polynomial model for SCWO of DURSET

Source	Sum of squares	Degree of freedom	Mean square	<i>F</i> -Value	<i>P</i> -value
Model	333.52	9	37.06	57.84	< 0.0001
<i>T</i> -temperature	177.76	1	177.76	277.44	< 0.0001
<i>t</i> -reaction time	54.13	1	54.13	84.49	< 0.0001
$\alpha$ -excess oxygen coefficient	34.19	1	34.19	53.37	< 0.0001
<i>Tt</i>	4.13	1	4.13	6.45	0.0294
<i>Tα</i>	1.06	1	1.06	1.65	0.2276
<i>tα</i>	0.0055	1	0.0055	0.0086	0.9279
<i>T</i> <sup>2</sup>	43.16	1	43.16	67.36	< 0.0001
<i>t</i> <sup>2</sup>	31.55	1	31.55	49.24	< 0.0001
$\alpha$ <sup>2</sup>	8.10	1	8.10	12.64	0.0052
Residual	6.41	10	0.64		
Lack of fit	4.96	5	0.99	3.43	0.1014
Pure error	1.45	5	0.29		
Cor total	339.93	19			

$R^2 = 0.9812$ ,  $R^2_{\text{adj}} = 0.9642$ ,  $R^2_{\text{pred}} = 0.8720$ , Adequate precision = 29.42,

$CV = 0.86\%$ ,  $SD = 0.80$

affecting the CRE was temperature > reaction time > excess oxygen coefficient. Compared with the pure error, the “lack of fit *F*-value” of 3.43 and its *P*-value of 0.1014 imply that the lack of fit was insignificant. In other words, there was a 10.14% possibility of noise influence caused by such a lack of fit value. The coefficient of determination ( $R^2$ ) and its adjusted value ( $R^2_{\text{adj}}$ ) were 0.9812 and 0.9642, respectively, proving that the correlation between the

experimental and predicted values was very high. The signal-to-noise ratio (Adeq. Precision) was 29.42. Usually, the signal-to-noise ratio is required to be greater than four, indicating that this multiple model can accurately reflect the experimental results [45]. Smaller coefficients of variation (*CV*) of multiple models lead to higher accuracy. The value of *CV* was 0.86% (< 5%), implying that the model was accurate and reliable [40].



### 3.3 Interactive effects of process parameters on responses

To better understand the three independent variables and their interactions, response plots provide a statistical

method to visually predict the relationship between the response and experimental level [46]. Figure 8 presents the response surface (3D) plots and contour plots that signify the interactive effect of multiple variables on the CRE obtained by the SCWO treatment of DURSET.

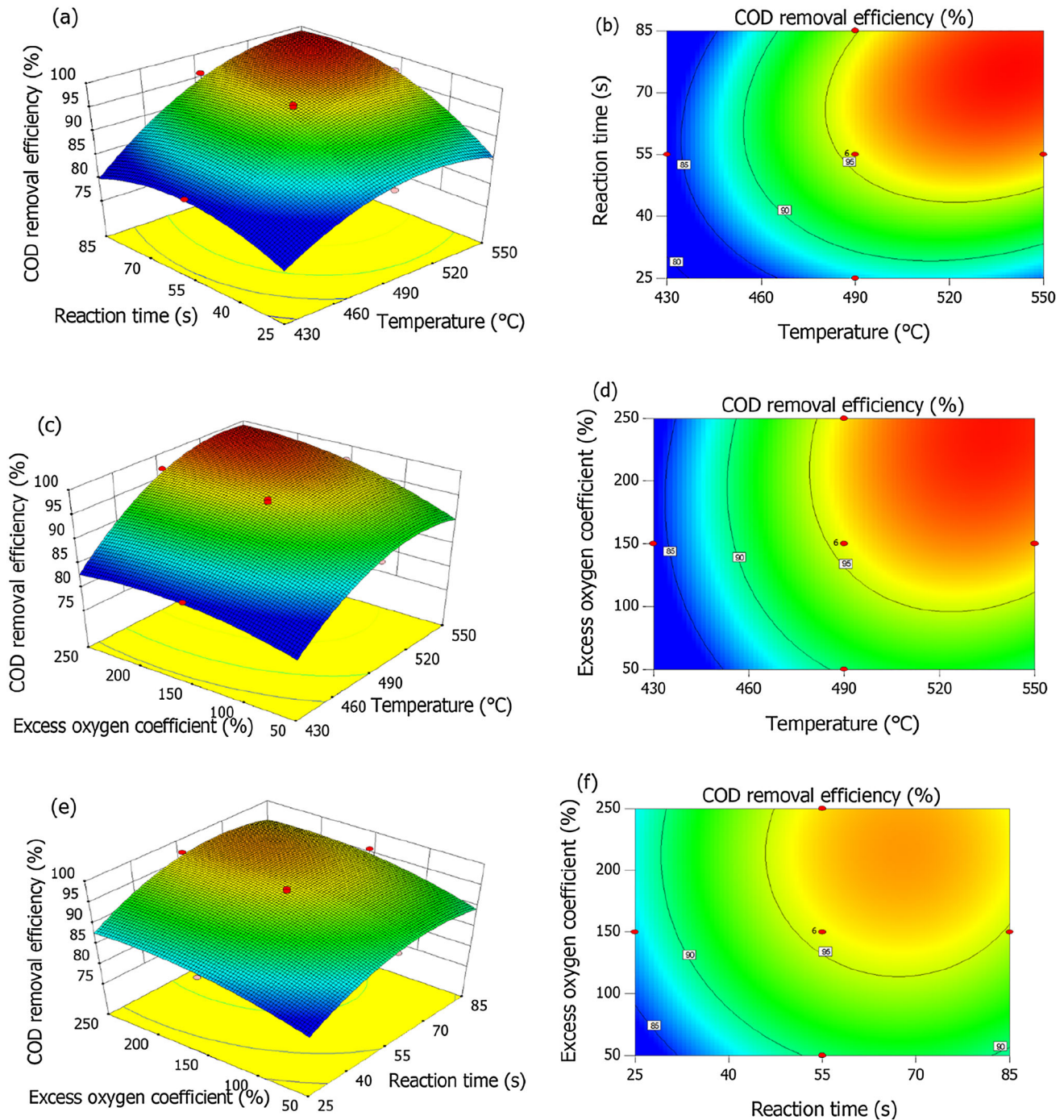


**Fig. 8** Three-dimensional and contour plots showing the interactive effects of **a, b** temperature and reaction time at excess oxygen coefficient of 150%, **c, d** temperature and excess oxygen coefficient at

reaction time of 55 s, **e, f** reaction time and excess oxygen coefficient at temperature of 490 °C on COD removal efficiency of DURSET

### 3.3.1 Interactive effect of temperature and reaction time

Figure 8a and b shows the interactive influence of temperature and reaction time on the CRE at excess oxygen coefficient of 150%. When the amount of oxidant was constant, CRE increased with increasing temperature and reaction time. Similar results have been reported in the literature [16, 47]. However, the effect of temperature on the CRE was greater than that of the reaction time, and the curve was steeper. This may be because increasing the temperature was helpful in increasing the number of activated molecules, thereby increasing the reaction rate. When the temperature increased from 430 to 550 °C, and the reaction time went up from 25 to 85 s, the CRE rose from 78.38 to 99.06%. It tended to increase sharply at first, and then slowly increase. This phenomenon can be explained by the three steps of the free-radical reaction mechanism: initiation, proliferation, and termination. Under SCW conditions,  $\text{H}_2\text{O}_2$  and  $\text{H}_2\text{O}$  rapidly decompose into free radicals. In the proliferation stage, a large number of free radicals produced in the initial stage attacked the organic molecular structure. As the reaction time increased, the termination phase gradually dominated. Finally, the generated refractory compounds may further impede COD removal of organic substances [48].

### 3.3.2 Interactive effect of temperature and excess oxygen coefficient

Figure 8c and d shows the interactive influence of temperature and excess oxygen coefficient on the CRE at the reaction time of 55 s. When the excess oxygen coefficient was greater than 50% and the temperature increased from 430 to 550 °C, the CRE increased by approximately 20%. This indicated that when the reaction time was constant, the interaction between temperature and oxidant could significantly promote the COD removal of organic matter. This was due to the fact that temperature played a major role in the SCWO of organic matter [22]. However, the COD removal was obviously slowed down when the temperature was greater than approximately 500 °C. This was because the organic matter was sufficiently oxidized, but the increase in temperature caused the water density and reactant concentration to decrease, thereby causing a decrease in the reaction rate and a slow increase in the CRE [49].

### 3.3.3 Interactive effect of reaction time and excess oxygen coefficient

The interaction between reaction time and excess oxygen coefficient on the CRE at the temperature of 490 °C is shown in Fig. 8e and f. As can be seen, the excess oxygen

coefficient had a relatively weak impact on the CRE than the reaction time, and with the rise of the reaction time, the CRE grew from 82.30 to 97.19%. From this, when the temperature was constant below 490 °C, the oxidative degradation of organic matter was incomplete. Additionally, the continuous increase in the reaction time and excess oxygen coefficient had no significant effect on COD removal when it exceeded a certain value. This may be due to the use of excess oxidant. The  $\text{HO}\cdot$  decomposed by hydrogen peroxide in the reaction system was already close to saturation; therefore, there was only a slight increase in the CRE. Hence, increasing temperature can help to improve the COD removal of organic matter.

## 3.4 Optimization and verification of process conditions

The optimal combination of various influencing factors in the reaction process can be obtained using RSM. Usually, in the optimization and selection of a combination of independent variables that meet the objective experimental conditions, the maximum CRE will be obtained in the supercritical water oxidation treatment of DURSET. Therefore, the CRE was selected to be “maximized”, while the independent factors were set to be “in range.” Table 6 presents the solution optimized via Design Expert 8.0.6 software, where the optimal process conditions were 515.03 °C, 66.33 s and an excess oxygen coefficient of 211.38%. However, considering the operability of the experiment, the optimum process conditions were 515 °C, 66 s, and excess oxygen coefficient 211%. These levels of process conditions led to a maximum removal rate of approximately 100%. To verify the agreement between predicted values and experimental values, three parallel experiments were conducted applying the optimum process conditions: the CRE of DURSET was  $99.49 \pm 0.23\%$ , and the COD concentration of liquid effluent was  $84.32 \pm 38.03 \text{ mg}\cdot\text{L}^{-1}$ . The error between the experimental and the predicted values was less than 1%, which indicates that the parameters of SCWO treatment of DURSET optimized by response surface analysis method are reliable, and the prediction is feasible according to the regression model.

## 3.5 Product analysis for SCWO of DURSET

In this section, the reaction intermediate products formed by the decomposition of DURSET in SCW are analyzed. The compounds extracted from the liquid effluent were separated and identified using GC/MS. The identification of reaction products at different retention times (RT) was achieved by comparing with the standard MS library (NIST 11). Table 7 lists major reaction

**Table 6** Optimized process conditions

Process conditions	Temperature (°C)	Reaction time (s)	Excess oxygen coefficient (%)	COD removal efficiency (%)
Values	515.03	66.33	211.38	100

**Table 7** Liquid products identified by GC/MS analysis obtained at 440 °C, 70 s, and excess oxygen coefficient of 50%

No	RT (min)	Compounds	Peak area (%)
1		Ketones	39.64
	5.28	Acetone	18.83
	7.57	2-Butanone	3.64
	9.01	2-Pentanone	6.28
	12.01	2-Hexanone	4.59
	18.56	Cyclohexanone	1.25
2	3.93	Ethyl ether	26
3		Benzene compounds	8.35
	8.11	Benzene	2.96
	10.72	Toluene	0.52
	23.41	Benzaldehyde	1.71
	24.95	4-Methylbenzaldehyde	1.32
	29.28	2-Methylphenol	1.54
4	8.49	Ethyl propionate	6.09
5	21.97	Acetic acid	3.05
6	3.7	Isopentane	2.83
7	26.58	Naphthalene	0.81
		Others	13.23

products identified from the SCWO of DURSET conducted at 440 °C, 70 s an excess oxygen coefficient 50%. As shown in Table 7, the main intermediate products were ketones, ethyl ether, benzene compounds, ethyl propionate, and others. Among these products, cyclic ketones and benzenes were considered refractory products, which mainly hindered the decomposition of organic matter and COD removal. It was worth mentioning that the newly produced naphthalene may be produced by dehydrogenation of decalin [50]. In addition, under special conditions, the phenyl radical of SCWO may generate dimers or polycyclic compounds such as naphthalene and phenanthrene through coupling reactions [17]. The mechanism of oxidative degradation is very complex and cannot be explained in detail through simple experiments. Cyclohexane in the stock solution can be oxidized to cyclic ketones under certain circumstances [51, 52]. Previous studies have shown that aromatic compounds (such as benzene, phenol, and naphthalene) are often regarded as

dominant intermediates that hinder the degradation reaction in SCW [26, 53]. Therefore, ketone and benzene compounds may be important intermediate products in the degradation process. In other words, the work in this section provides a basis for further study on the degradation mechanism of oil cleaning agents treated by SCWO.

## 4 Conclusion

This study demonstrates that SCWO is an effective green technology for the treatment of DURSET oil cleaning agents from nuclear power plants. In this study, the experimental design and optimization of the SCWO degradation of oil cleaning agents were realized via RSM. The following conclusions were drawn:

- (1) Through single-factor experimental analysis, the main influencing factors (including temperature, reaction time, and excess oxygen coefficient) were determined for the follow-up response surface scheme design. The optimized value range of these main factors was selected as a temperature range of 430–550 °C, reaction time of 25–85 s, and an excess oxygen coefficient range of 50–250%.
- (2) A polynomial equation model for predicting COD removal, involving three independent variables, was established. The coefficient of determination ( $R^2$ ) was 0.9812, demonstrating that the proposed predictive model was adequate. This temperature was found to be the main factor affecting the SCWO process.
- (3) The optimal reaction conditions at a pressure of 24 MPa and feed concentration of 2 wt% were determined to be at 515 °C, 66 s, and an excess oxygen coefficient of 211%. Under these conditions, the CRE of DURSET was up to 99.5%, the COD of liquid effluent was less than 100 mg·L<sup>-1</sup>, and with a standard deviation of less than 1%. These results further confirm the reliability of the quadratic empirical equation model.
- (4) Product analysis of the liquid effluent using GC/MS revealed that ketones and benzene compounds may be the main intermediates of DURSET in the process



of oxidative degradation by supercritical water. This work provides a foundation for the study and development of SCWO treatment of spent radioactive organic solvents.

**Author contributions** All authors contributed to the study conception and design. Material preparation, data collection, and analysis were performed by Xiao-Bin Xia, Shi-Bin Li, Qiang Qin, Shuai - Wang, and Hong-Jun Ma. The first draft of the manuscript was written by Shi-Bin Li, and all authors commented on previous versions of the manuscript. All authors read and approved the final manuscript.

## References

1. R. Rahman, H.A. Ibrahim, Y.T. Hung, Liquid radioactive wastes treatment: a review. *Water* **3**(4), 551–565 (2011). <https://doi.org/10.3390/w3020551>
2. M. Mabrouk, F. Lemont, J.M. Baronne, Incineration of radioactive organic liquid wastes by underwater thermal plasma. *J. Phys. Conf. Ser.* **406**, 012002 (2012). <https://doi.org/10.1088/1742-6596/406/1/012002>
3. J. Deckers, Incineration and plasma processes and technology for treatment and conditioning of radioactive waste. In *Handbook of Advanced Radioactive Waste Conditioning Technologies* (2011), pp. 43–66. <https://doi.org/10.1533/9780857090959.1.43>
4. V. Cuccia, C.B. Freire, A.C.Q. Ladeira, Radwaste oil immobilization in geopolymer after non-destructive treatment. *Prog. Nucl. Energ.* **122**, 103246 (2020). <https://doi.org/10.1016/j.pnuene.2020.103246>
5. W. Zhang, J. Wang, Leaching performance of uranium from the cement solidified matrices containing spent radioactive organic solvent. *Ann. Nucl. Energy* **101**, 31–35 (2017). <https://doi.org/10.1016/j.anucene.2016.09.055>
6. W.A. Chao, B. Gya, B. Jwa, Fenton oxidative degradation of spent organic solvents from nuclear fuel reprocessing plant. *Prog. Nucl. Energ.* **130**, 103563 (2020). <https://doi.org/10.1016/j.pnuene.2020.103563>
7. M. Takai, M. Aoyama, O. Nakazawa et al., Steam reforming: alternative pyrolytic technology to incineration for volume reduction and stabilization of low-level radioactive organic liquid wastes. *J. Phys. Chem. Solids* **66**(2–4), 694–696 (2005). <https://doi.org/10.1016/j.jpcs.2004.07.025>
8. U. Galla, P. Kritzer, J. Bringmann et al., Process for total degradation of organic wastes by mediated electrooxidation. *Chem. Eng. Technol.* **23**(3), 230–233 (2000). [https://doi.org/10.1002/\(sici\)1521-4125\(200003\)23:3%3c230::aid-ceat230%3e3.0.co;2-3](https://doi.org/10.1002/(sici)1521-4125(200003)23:3%3c230::aid-ceat230%3e3.0.co;2-3)
9. Q. Wu, X. Hu, P.L. Yue, Kinetics study on catalytic wet air oxidation of phenol. *Chem. Eng. Sci.* **58**(3), 923–928 (2003). [https://doi.org/10.1016/S0009-2509\(02\)00628-0](https://doi.org/10.1016/S0009-2509(02)00628-0)
10. P.E. Savage, Organic chemical reactions in supercritical water. *Chem. Rev.* **99**(2), 603–622 (1999). <https://doi.org/10.1021/cr9700989>
11. Q. Qin, X.B. Xia, S.B. Li et al., Supercritical water oxidation and its application in radioactive waste treatment. *Ind. Water Treat.* 1–16 (2021). <https://doi.org/10.19965/j.cnki.iwt.2021-0855> (in Chinese)
12. P. Kritzer, E. Dinjus, An assessment of supercritical water oxidation (SCWO): Existing problems, possible solutions and new reactor concepts. *Chem. Eng. J.* **83**(3), 207–214 (2001). [https://doi.org/10.1016/S1385-8947\(00\)00255-2](https://doi.org/10.1016/S1385-8947(00)00255-2)
13. Q. Qin, S. Wang, H.Y. Wang et al., Treatment of radioactive spent extraction solvent by supercritical water oxidation. *J. Radioanal. Nucl. Ch.* **314**(2), 1169–1176 (2017). <https://doi.org/10.1007/s10967-017-5445-1>
14. T.Z. Ma, T.T. Hu, D.D. Jiang et al., Treatment of penicillin with supercritical water oxidation: experimental study of combined ReaxFF molecular dynamics. *Korean J. Chem. Eng.* **35**(4), 900–908 (2018). <https://doi.org/10.1007/s11814-017-0341-5>
15. S.V.P. Mylapilli, S.N. Reddy, Sub and supercritical water oxidation of pharmaceutical wastewater. *J. Environ. Chem. Eng.* **7**(3), 103165 (2019). <https://doi.org/10.1016/j.jece.2019.103165>
16. J. Li, S. Wang, Y. Li et al., Supercritical water oxidation of semi-coke wastewater: effects of operating parameters, reaction mechanism and process enhancement. *Sci. Total Environ.* **710**, 134396 (2020). <https://doi.org/10.1016/j.scitotenv.2019.134396>
17. S.J. Chang, Y.C. Liu, Degradation mechanism of 2,4,6-trinitrotoluene in supercritical water oxidation. *J. Environ. Sci.* **19**(12), 1430–1435 (2007). [https://doi.org/10.1016/S1001-0742\(07\)60233-2](https://doi.org/10.1016/S1001-0742(07)60233-2)
18. Y.M. Gong, Y. Guo, J.D. Sheehan et al., Oxidative degradation of landfill leachate by catalysis of CeMnOx/TiO<sub>2</sub> in supercritical water: mechanism and kinetic study. *Chem. Eng. J.* **331**, 578–586 (2018). <https://doi.org/10.1016/j.cej.2017.08.122>
19. J. Li, S. Wang, Y. Li et al., Supercritical water oxidation of glyphosate wastewater. *Chem. Eng. Res. Des.* **168**, 122–134 (2021). <https://doi.org/10.1016/j.cherd.2021.02.002>
20. P.A. Marrone, Supercritical water oxidation-current status of full-scale commercial activity for waste destruction. *J. Supercrit. Fluid.* **79**, 283–288 (2013). <https://doi.org/10.1016/j.supflu.2012.12.020>
21. T. Xu, S. Wang, Y. Li et al., Review of the destruction of organic radioactive wastes by supercritical water oxidation. *Sci. Total Environ.* **799**, 149396 (2021). <https://doi.org/10.1016/j.scitotenv.2021.149396>
22. T.T. Xu, S.Z. Wang, Y.H. Li et al., Optimization and mechanism study on destruction of the simulated waste ion-exchange resin from the nuclear industry in supercritical water. *Ind. Eng. Chem. Res.* **59**(40), 18269–18279 (2020). <https://doi.org/10.1021/acs.iecr.0c02732>
23. M. Kosari, M. Golmohammadi, J. Towfighi et al., Decomposition of tributyl phosphate at supercritical water oxidation conditions: Non-catalytic, catalytic, and kinetic reaction studies. *J. Supercrit. Fluid.* **133**, 103–113 (2018). <https://doi.org/10.1016/j.supflu.2017.09.012>
24. M. Golmohammadi, S.J. Ahmadi, J. Towfighi, Catalytic supercritical water destructive oxidation of tributyl phosphate: Study on the effect of operational parameters. *J. Supercrit. Fluid.* **140**, 32–40 (2018). <https://doi.org/10.1016/j.supflu.2018.05.022>
25. A. Leybros, A. Roubaud, P. Guichardon et al., Supercritical water oxidation of ion exchange resins: degradation mechanisms. *Process Saf. Environ.* **88**(3), 213–222 (2010). <https://doi.org/10.1016/j.psep.2009.11.001>
26. L. Wang, L. Yi, G. Wang et al., Experimental investigation on gasification of cationic ion exchange resin used in nuclear power plants by supercritical water. *J. Hazard. Mater.* **419**, 126437 (2021). <https://doi.org/10.1016/j.jhazmat.2021.126437>
27. S. Wang, Q. Qin, K. Chen et al., Supercritical water oxidation of spent extraction solvent simulants. *Nucl. Sci. Tech.* **26**(3), 030601 (2015). <https://doi.org/10.13538/j.1001-8042/nst.26.030601>
28. Q. Qin, S. Wang, H. Peng et al., Solubility of inorganic salt in supercritical water. *J. Radioanal. Nucl. Ch.* **317**(2), 947–957 (2018). <https://doi.org/10.1007/s10967-018-5939-5>

29. S.B. Li, X.B. Xia, Q. Qin et al., Experimental study on supercritical water oxidation of lubricating oil from nuclear power plant. *Nucl. Tech.* **44**(07), 91–98 (2021). <https://doi.org/10.11889/j.0253-3219.2021.hjs.44.070603> (in Chinese)
30. X.R. Huang, Application of response surface method on biological process optimization. Hunan University (2011). <https://kns.cnki.net/KCMS/detail/detail.aspx?dbname=CMFD201301&file name=1012492463.nh> (in Chinese)
31. M. Mäkelä, Experimental design and response surface methodology in energy applications: a tutorial review. *Energy Convers. Manag.* **151**, 630–640 (2017). <https://doi.org/10.1016/j.enconman.2017.09.021>
32. C.M. Huelsman, P.E. Savage, Intermediates and kinetics for phenol gasification in supercritical water. *Phys. Chem. Chem. Phys.* **14**(8), 2900–2910 (2012). <https://doi.org/10.1039/c2cp23910h>
33. B.W. Yang, Z.W. Cheng, X.P. Gao et al., Decomposition of 15 aromatic compounds in supercritical water oxidation. *Chemosphere* **218**, 384–390 (2019). <https://doi.org/10.1016/j.chemosphere.2018.11.048>
34. B. Al-Duri, L. Pinto, N.H. Ashraf-Ball et al., Thermal abatement of nitrogen-containing hydrocarbons by noncatalytic supercritical water oxidation (SCWO). *J. Mater. Sci.* **43**(4), 1421–1428 (2008). <https://doi.org/10.1007/s10853-007-2285-3>
35. N. Wei, D.H. Xu, B.T. Hao et al., Chemical reactions of organic compounds in supercritical water gasification and oxidation. *Water Res.* **190**, 116634 (2021). <https://doi.org/10.1016/j.watres.2020.116634>
36. W. Bühler, E. Dinjus, H.J. Ederer et al., Ionic reactions and pyrolysis of glycerol as competing reaction pathways in near- and supercritical water. *J. Supercrit. Fluid* **22**(1), 37–53 (2002). [https://doi.org/10.1016/S0896-8446\(01\)00105-X](https://doi.org/10.1016/S0896-8446(01)00105-X)
37. L. Yu, Y.H. Chen, F. He, catalytic supercritical water oxidation of oily wastewater. *Chem. Tech. Fuels Oil* **51**(1), 87–92 (2015). <https://doi.org/10.1007/s10553-015-0578-3>
38. Z. Chen, Z.L. Chen, F.J. Yin et al., Supercritical water oxidation of oil-based drill cuttings. *J. Hazard. Mater.* **332**, 205–213 (2017). <https://doi.org/10.1016/j.jhazmat.2017.03.001>
39. Y.M. Gong, Y. Guo, S.Z. Wang et al., Supercritical water oxidation of Quinazoline: effects of conversion parameters and reaction mechanism. *Water Res.* **100**, 116–125 (2016). <https://doi.org/10.1016/j.watres.2016.05.001>
40. Y. Gong, S. Wang, H. Xu et al., Partial oxidation of landfill leachate in supercritical water: optimization by response surface methodology. *Waste Manag.* **43**, 343–352 (2015). <https://doi.org/10.1016/j.wasman.2015.04.013>
41. M. Wahyudiono, M. Sasaki, Goto, kinetic study for liquefaction of tar in sub- and supercritical water. *Polym. Degrad. Stabil.* **93**(6), 1194–1204 (2008). <https://doi.org/10.1016/j.polydegradstab.2008.02.006>
42. A.G. Chakinala, S. Kumar, A. Kruse et al., Supercritical water gasification of organic acids and alcohols: the effect of chain length. *J. Supercrit. Fluid.* **74**, 8–21 (2013). <https://doi.org/10.1016/j.supflu.2012.11.013>
43. M. Hosseinpour, M. Soltani, A. Noofeli et al., An optimization study on heavy oil upgrading in supercritical water through the response surface methodology (RSM). *Fuel* **271**, 117618 (2020). <https://doi.org/10.1016/j.fuel.2020.117618>
44. J. Zhang, J. Lu, S. Chen et al., Experimental and kinetics study on oxidation of three-component in supercritical water. *Can. J. Chem. Eng.* **97**(6), 1871–1880 (2019). <https://doi.org/10.1002/cjce.23454>
45. N. Aghamohammadi, H.B. Aziz, M.H. Isa et al., Powdered activated carbon augmented activated sludge process for treatment of semi-aerobic landfill leachate using response surface methodology. *Bioresour. Technol.* **98**(18), 3570–3578 (2007). <https://doi.org/10.1016/j.biortech.2006.11.037>
46. M. Ravber, Ž. Knez, M. Škerget, Optimization of hydrolysis of rutin in subcritical water using response surface methodology. *J. Supercrit. Fluid.* **104**, 145–152 (2015). <https://doi.org/10.1016/j.supflu.2015.05.028>
47. Z. Yan, B. Örmeci, Y. Han et al., Supercritical water oxidation for treatment of wastewater sludge and recalcitrant organic contaminants. *Environ. Technol. Innov.* **18**, 100728 (2020). <https://doi.org/10.1016/j.eti.2020.100728>
48. S. Gopalan, P.E. Savage, A reaction network model for phenol oxidation in supercritical water. *Aiche J.* **41**(8), 1864–1873 (1995). <https://doi.org/10.1002/aic.690410805>
49. X.Q. Dong, Z.D. Gan, X.L. Lu et al., Study on catalytic and non-catalytic supercritical water oxidation of p-nitrophenol wastewater. *Chem. Eng. J.* **277**, 30–39 (2015). <https://doi.org/10.1016/j.cej.2015.04.134>
50. S. Xu, I. Butler, I. Gkalp et al., Evolution of naphthalene and its intermediates during oxidation in subcritical/supercritical water. *P. Combust. Inst.* **33**(2), 3185–3194 (2011). <https://doi.org/10.1016/j.proci.2010.09.010>
51. Y.B. She, J.H. Deng, L. Zhang et al., Catalytic oxidation of cyclohexane by O<sub>2</sub> as an oxidant. *Prog. Chem.* **30**(01), 124–136 (2018). <https://doi.org/10.7536/PC171102>
52. N.H. Attanayake, M. Tang, Performance and pathways of electrochemical cyclohexane oxidation. *Curr. Opin. Electrochem.* **30**, 100791 (2021). <https://doi.org/10.1016/j.coelec.2021.100791>
53. G.J. Dileo, M.E. Neff, P.E. Savage, Gasification of guaiacol and phenol in supercritical water. *Energ. Fuel.* **21**(4), 2340–2345 (2007). <https://doi.org/10.1021/ef070056f>